Received: 20 December 2023 | Revised: 12 March 2024 | Accepted: 10 April 2024

DOI: 10.1111/psyp.14596

PSYCHOPHYSIOLOGY SPR WILEY

ORIGINAL ARTICLE

Gray matter matters: Cognitive stability and flexibility in schizophrenia spectrum disorder

Florentine Herkströter[1] | **Anoushiravan Zahedi**[2,3] | **Isabel Standke**[4] | **Udo Dannlowski**[2,4] | **Rebekka Lencer**[4,5] | **Ricarda I. Schubotz**[2,3] | **Ima Trempler**[2,3]

[1]Department of Neurology, Niels-Stensen-Kliniken, Marienhospital Osnabrück-Standort Natruper Holz, Osnabrueck, Germany

[2]Institute of Psychology, University of Muenster, Muenster, Germany

[3]Otto Creutzfeldt-Center for Cognitive and Behavioral Neuroscience, University of Muenster, Muenster, Germany

[4]Institute for Translational Psychiatry, University of Muenster, Muenster, Germany

[5]Department of Psychiatry and Psychotherapy, University of Luebeck, Luebeck, Germany

Correspondence
Anoushiravan Zahedi, Institute of Psychology, University of Muenster, Fliednerstr. 21, Muenster 48149, Germany.
Email: azahedi@uni-muenster.de

Florentine Herkströter, Department of Neurology, Niels-Stensen-Kliniken, Marienhospital Osnabrück-Standort Natruper Holz, Am Natruper Holz 69, Osnabrueck 49076, Germany.
Email: florentine.herkstroeter@magenta.de

Funding information
Medical Faculty of the University of Muenster; Deutsche Forschungsgemeinschaft, Grant/Award Number: FOR2107 DA1151/5-1, DA1151/5-2, SFB-TRR58, C09 and Z02; the Interdisciplinary Center for Clinical Research (IZKF) of the Medical Faculty of the University of Muenster, Grant/Award Number: Dan3/012/17

Abstract

Cognitive dysfunction constitutes a core characteristic of schizophrenia spectrum disorders (SZ). Specifically, deficits in updating generative models (i.e., *cognitive flexibility*) and shielding against distractions (i.e., *cognitive stability*) are considered critical contributors to cognitive impairment in these patients. Here, we examined the structural integrity of frontostriatal networks and their associations with reduced cognitive stability and flexibility in SZ patients. In a sample of 21 patients diagnosed with SZ and 22 healthy controls, we measured gray matter volume (GMV) using structural MRI. Further, cognitive stability and flexibility were assessed using a switch-drift paradigm, quantifying the successful ignoring of distracters and detection of rule switches. Compared to controls, patients showed significantly smaller GMV in the whole brain and three predefined regions of interest: the medial prefrontal cortex (mPFC), inferior frontal gyrus (IFG), and caudate nucleus (CN). Notably, GMV in these areas positively correlated with correct rule-switch detection but not with ignoring rule-compatible drifts. Further, the volumetric differences between SZ patients and controls were statistically explainable by considering the behavioral performance in the switch-drift task. Our results indicate that morphological abnormalities in frontostriatal networks are associated with deficient flexibility in SZ patients and highlight the necessity of minimizing neurodevelopmental and progressive brain atrophy in this population.

Florentine Herkströter and Anoushiravan Zahedi contributed equally to this work.

KEYWORDS
cognitive stability and flexibility, frontostriatal networks, gray matter volume, prediction errors, schizophrenia

1 | INTRODUCTION

Cognitive impairment represents a core characteristic of schizophrenia spectrum disorders (SZ; Bowie & Harvey, 2005; Lepage et al., 2014). Considering that diminished cognitive performance is associated with disrupted everyday functioning and poorer clinical outcomes (Lepage et al., 2014), fostering our understanding of cognitive impairment in SZ is crucial for developing better treatment options for these patients. It has been suggested that deficits in shielding distracters, i.e., *cognitive stability*, and adapting to contextual changes, i.e., *cognitive flexibility*, contribute to impairment in various cognitive domains observed in SZ (Braver et al., 1999). Notably, stabilizing and flexible updating of internal models rely on the integrity of several partially overlapping brain networks in which frontostriatal areas play an essential role (Armbruster et al., 2012; Cadena et al., 2018, 2019; Floresco et al., 2009; Jiang et al., 2015; Trempler et al., 2017). Given that reduced gray matter volume (GMV) is well documented in patients with SZ (for a meta-analysis, see Gupta et al., 2015; Haijma et al., 2013; Williams, 2008), with studies showing brain atrophy even before the onset of psychosis as well as progressive degeneration over time (Dietsche et al., 2017; Veijola et al., 2014), it is vital to understand the relationship between GMV and SZ patients' cognitive impairments. After showing the relationships between deficits in cognitive stability and flexibility with functional neural responses in SZ patients in our previous work (Standke et al., 2021), in the current study, we investigated the relationship between anatomical brain structure and cognitive stability and flexibility in SZ patients compared to a neurotypical control group.

Even though previous studies showed a general decline in GMV in SZ patients, it is unclear whether GMV losses in specific regions of interest (ROIs) relate to deficient predictive processing in these patients. Our previous works on healthy subjects and patients with SZ using functional MRI corroborated the notion that cognitive flexibility and stability rely on dopamine-mediated frontostriatal loops (Standke et al., 2021; Trempler et al., 2017). Specifically, we found that reduced striatal activation was associated with impaired cognitive stability and flexibility in patients with SZ, suggesting that striatal gating to the frontal cortex might be disrupted (Standke et al., 2021; Trempler et al., 2017). The striatum, including its subregions, i.e., the caudate nucleus (CN) and putamen, are known to be crucially involved in gating prediction errors (Chatham & Badre, 2015) caused by novelty or cognitive surprise (Diederen & Fletcher, 2021; McCutcheon et al., 2019). Theories propose that phasic release of striatal dopamine attributes salience to currently relevant information by activating striatal D2 receptors supporting flexible updating, thereby triggering the frontal cortex to engage (Frank et al., 2001). On the other hand, lower dopamine concentrations activate D1 receptors that foster stabilization by closing the gate to the frontal cortex (O'Reilly, 2006). Hence, the striatum determines which information gets passed on to the cortex using so-called go and nogo pathways. Thus, striatal dysfunction may underlie aberrant weighting and signaling of prediction errors, thereby impairing the stability and flexibility of predictions in SZ. Nevertheless, previous studies show mixed results regarding striatal GMV in SZ patients, as some suggest an increase (Sigmundsson et al., 2001; Simpson et al., 2010; Williams, 2008), but others indicate a decrease in the striatum GMV (Koo et al., 2006; Perez-Costas et al., 2010).

Deficient cognitive instability and inflexibility in SZ also seem to relate to deficient cortical processing of prediction errors in frontal areas rather than to disrupted striatal gating only (Standke et al., 2021). Specifically, the inferior frontal gyrus (IFG) was shown to support stabilization of internal models against distraction (Standke et al., 2021; Trempler et al., 2017), consistent with its role in response inhibition and distractor resistance (e.g., Aron et al., 2014; Bilder et al., 2004; Schaum et al., 2021; Sharp et al., 2010; Wager et al., 2014). Flexible updating of predictions, on the other hand, was associated with the medial prefrontal cortex (mPFC) in patients with SZ (Standke et al., 2021) and healthy controls (Trempler et al., 2017). Intriguingly, several studies consistently identified frontal gray matter loss in patients with SZ, including the mPFC (Bonilha et al., 2008; Shepherd et al., 2012; Sigmundsson et al., 2001; Williams, 2008; Zhang et al., 2018) and the IFG (Antonova et al., 2005; Dietsche et al., 2017; Sigmundsson et al., 2001; Williams, 2008). Although preliminary research in patients with SZ provides some evidence linking prefrontal GMV loss to executive dysfunction (Jirsaraie et al., 2018) and cognitive perseverance (Bonilha et al., 2008), it is unclear whether cognitive flexibility and stability are related to these regional GMV losses.

To summarize, existing evidence points to (I) aberrant frontostriatal functioning underlying deficient cognitive stability and flexibility in patients with SZ and (II)

structural alterations in respective networks. However, it is unclear whether these morphological abnormalities contribute to deficient predictive processing in SZ (Standke et al., 2021). The current study addressed whether volumetric alterations of predefined frontostriatal areas (i.e., mPFC, IFG, and striatum) relate to reduced flexibility and stability in SZ, providing further evidence for dysfunctional frontostriatal networks as an essential underlying cause of cognitive impairment in SZ patients.

In order to independently assess cognitive flexibility and stability, a previously employed serial switch-drift-paradigm (Figure 1) was administered, requiring participants to react to switches of the underlying model and ignore transient omissions (Standke et al., 2021; Trempler et al., 2017, 2018). We hypothesized that GMV, extracted from T1 magnetic resonance images (MRI) collected before the task administration, would be attenuated in SZ patients compared to a healthy sample. Specifically, in SZ patients compared to the healthy control group, we expected reduced GMVs in predefined anatomical ROIs: mPFC, IFG, and striatum. Secondly, we hypothesized that these GMV losses in SZ patients can be predicted by performance in the switch-drift task.

2 | METHODS

2.1 | Participants

Our sample was the same as that reported in Standke et al. (2021) consisting of twenty-two patients (7 females; 36.41 ± 10.28 years old; range 24–57 years; 20 right-handed)

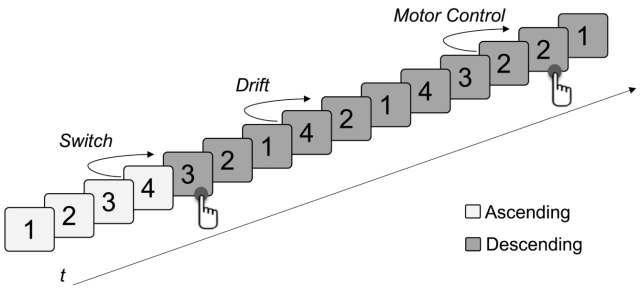

FIGURE 1 Serial switch-drift-paradigm. Schematic depiction of the task as previously employed by Standke et al. (2021). Sequences of four consecutive digits were presented continuously, either in an ascending or in a descending order. Occasionally, unexpected directional changes occurred (i.e., switches) that were to be indicated via button press, reflecting flexible updating of the current prediction (left). On the other hand, participants were asked to ignore omissions of single digits (i.e., drifts), requiring shielding of the internal model (middle). Finally, participants had to respond to repetitions of single digits by quickly pressing a key to determine the individual response window (motor control task, right).

diagnosed with schizophrenia or schizoaffective disorder (abbreviated as SZ in the following) and twenty-two healthy controls (9 females; 38.23 ± 12.26 years old; range 22–63 years; 19 right-handed). One patient diagnosed with schizoaffective disorder was excluded from analysis due to poor magnetic resonance imaging (MRI) data quality, as indicated by the weighted average image and preprocessing quality index (Gaser & Kurth, 2020), thereby leaving a total of 21 patients and 22 healthy controls for further analyses.

All patients were recruited at the Department of Mental Health of the University Hospital Muenster. Diagnoses were established at consensus conferences based on the structured Clinical Interview I for DSM-IV (SCID-I) (American Psychological Association, 1994) and further available clinical data. Patients participated under regular medication, with a mean converted chlorpromazine equivalent (CPZ; Andreasen et al., 2010) of 639.63 mg (±427.12). Eighteen patients were treated with atypical antipsychotic medication, one with typical antipsychotic medication, and three did not receive any antipsychotic medication. None of the patients were diagnosed with a neurological disorder. All patients with a history of substance abuse were at least four weeks abstinent before participating in the study. Healthy controls were recruited via advertisements. According to the screening questionnaire of SCID (Glasofer et al., 2015), none of the controls had a history of psychiatric illness. Moreover, they reported no known neurological disorders at the time of testing. Additionally, there was also no known history of psychiatric disorders in first-degree relatives of the controls. Every participant had a normal or corrected-to-normal vision.

The study procedures are in accordance with the Helsinki Declaration and were approved by the local ethics committee of the University of Muenster. Every participant gave written informed consent and was reimbursed for their participation.

2.2 | Assessment tools

The positive and negative symptoms of all participants were assessed using the Scale for the Assessment of Positive Symptoms (SAPS; Andreasen, 1984) and the Scale for the Assessment of Negative Symptoms (SANS; Andreasen, 1984), respectively. SAPS is a 34-item assessment tool that focuses on positive symptoms of schizophrenia in five different categories: hallucination, delusion, bizarre behavior, and positive formal thought disorder. The items are measured using a 6-point scale. Further, SANS comprises 25 items, measured using a 6-point scale, quantifying negative symptoms across five categories: affective blunting, alogia, avolition-apathy,

anhedonia-asociality, and inattention. Both tools are commonly used for assessing SZ symptoms for academic and clinical purposes and show high interrater reliability and moderate temporal stability (Andreasen & Olsen, 1982; Kumari et al., 2017).

Further, all participants completed the Heidelberg Scale for Neurological Soft Signs (NSS; Schroder et al., 1991), the Becks Depression Inventory II (BDI-II; Beck et al., 1996), and the Barratt Impulsiveness Scale (BIS; Patton et al., 1995). Notably, these questionnaires are not the subject of the current study and will be described and analyzed elsewhere.

2.3 | Paradigm and procedure

We employed a serial switch-drift paradigm (Trempler et al., 2017, 2018) designed to assess the stability and flexibility of predictions independently (Figure 1). Participants were shown a continuously presented ascending (1–2–3–4) or descending (4–3–2–1) four-digit sequence that enables participants to predict forthcoming digits based on two generated internal models (ascending or descending model). Numbers were presented successively, one at a time, at the center of the screen for one second with an inter-stimulus interval of 100 ms. Occasionally, unexpected directional changes, i.e., switches from an ascending to a descending sequence or vice versa, occurred at random positions within a series (i.e., switch), requiring the participant to adapt their prediction accordingly. Those switches between models were to be indicated by pressing a button as quickly as possible. Additionally, single digits were sometimes randomly omitted (i.e., drifts) without causing a temporal gap. Since the current model remained valid despite the omission, participants were asked to ignore those drifts, requiring the internal model to be stabilized against a transient violation of the prediction. Button presses were counted if they occurred within a response window defined by the mean individual reaction time plus one standard deviation. Individual mean reaction time was assessed via motor control condition, where repetitions of single digits had to be indicated by pressing a key. The targeted digit would be repeated (max. seven times) until a response was produced.

The task consisted of 12 blocks, with each containing 125 digits. Between each block, a fixation cross was presented for 6 s. The randomization was programmed using MATLAB R2012b (The MathWorks Inc., Natick, MA, USA), and stimuli were presented using Presentation 13.1 (Neurobehavioral Systems, San Francisco, CA, USA).

The day before the MRI session, all participants completed an instructed practice session consisting of ten blocks with 80 digits each to ensure participants understood the task. Moreover, every participant completed an additional short practice composed of three blocks immediately before the MRI session. All other assessments, including questionnaires and interviews, took place on a day within 1 week before the MRI session.

2.4 | Brain imaging acquisition

Brain imaging data of patients and controls were recorded using a 3 Tesla MRI Scanner (Magnetom Prisma, Siemens Medical Solutions, Erlangen, Germany) equipped with a 20-channel head coil. High-resolution structural images of the individual brain anatomy were obtained using a standard Siemens T1-weighted magnetization-prepared rapid acquisition with gradient echo (MPRAGE) sequence with isotropic voxels (1 × 1 × 1 mm) in a 256 mm field of view (256 × 265 pixels, 192 slices, repetition time = 2130, echo time = 2.28). In addition, blood-oxygen-level-dependent (BOLD) functional imaging was recorded using T2*-weighted single-shot, echoplanar-imaging (EPI) sequences (64 × 64 pixel, 210 mm field of view, 90° flip angle, repetition time = 2000 ms, echo time = 30 ms). Here we focus on T1 images and the structural properties extracted from them, whereas the functional analyses are reported by Standke et al. (2021).

2.5 | Structural images pre-processing and voxel-based morphometry

Imaging data was pre-processed using the Statistical Parametric Mapping (SPM) software 12 (Wellcome Department of Imaging Neuroscience, London, UK) as well as the Computational Anatomy Toolbox 12 (CAT12; Gaser et al., 2020) implemented in SPM12. Both programs were run in MATLAB version 2023a. Initially, all images were converted from DICOM into NIFTI format. Each image was reoriented to the same point of origin (anterior commissure) and registered to a standard brain (single subject T1). All images were inspected for artifacts prior to segmentation. Further pre-processing was performed using CAT12. Segmentation consisted of two fully automated standardized voxel-based processing steps. First, MRI data was denoised using a spatial adaptive non-local means (SANLM) denoising filter, internally resampled, corrected for bias, affine registered, and segmented. Second, refined processing of these images entailed the removal of non-brain tissue (skull-stripping), brain parcellation (left and right hemisphere, subcortical areas, cerebellum), and local intensity correction. The final segmentation followed an adaptive maximum a posteriori (AMAP) approach with partial volume

model estimation, resulting in three tissue types: gray matter, white matter, and cerebrospinal fluids. Finally, all tissue components were spatially normalized to a common reference space (MNI) using the Diffeomorphic Anatomical Registration Through Exponentiated Lie (DARTEL) algebra algorithm. A data quality check was performed, showing good overall data quality, with the mean data quality being 85.35% ($\pm$0.85). However, after visual inspection for outliers using a boxplot, one patient had to be excluded due to poor data quality (74.69%, more than 3 *SD* below the mean). Patients and controls did not differ in image quality ($U = 236.5, p = .894; z = 0.13$). Further inspection of data homogeneity yielded no severe abnormalities.

Voxel-based morphometry (VBM) analysis was performed using CAT12 following the recommended standard protocol (Gaser & Kurth, 2020). The significance threshold was set to a false discovery rate (FDR) of 0.05 ($p_{\text{FDR-corrected}} = .05$). The absolute masking threshold was set to 0.1 as recommended. Each participant's modulated and normalized gray data was smoothed using an 8-mm full width at half maximum Gaussian filter. Total intracranial volume (TIV) and total GMV were extracted. Additionally, based on the volume-based mori atlas (Oishi et al., 2009), GMVs of the following anatomical ROIs were extracted for further ROI analyses: mPFC, IFG, and two subregions of the striatum (i.e., putamen and caudate nucleus). GMV of mPFC was determined by summing the volumes of the cingulate gyrus and the superior frontal gyrus in accordance with previous studies (Trempler et al., 2018). All volumes were averaged over both hemispheres, as we did not define specific hypotheses regarding laterality.

2.6 | Statistical analyses

All statistical analyses were conducted via the R programming language (http://www.R-project.org/), MATLAB (r2023b; MathWorks Company), and SPM12 (The Wellcome Department of Imaging Neuroscience, Institute of Neurology, London, UK). Unpaired *t* tests and nonparametric Mann–Whitney *U*-tests (in the case of nonnormally distributed data) were computed to investigate differences between patients and controls regarding demographics and clinical characteristics. The distributions of gender and handedness between the two groups were compared using chi-square tests.

In order to investigate VBM results and the relationships between VBM and behavioral results, Bayesian multivariate linear regression modeling (BMLM) was used. Before analysis, all variables were checked for normal distribution using the Shapiro–Wilk test and by visual inspection of QQ plots. Further, the data was checked for any extreme outliers [i.e., outside Quartile 1 (Q1) $-$ 3 $*$ interquartile (IQR), Q3 + 3 $*$ IQR]. Volumetric analyses were divided into two parts: first, the whole brain analysis was conducted using both SPM and separate Bayesian general linear modeling (BLM). Second, a region-of-interest-volumetric analysis was conducted to address the changes in the a-priori-defined ROIs., For analyzing the VBM results, TIV, gender, and age were used as nuisance variables based on the recommendation of Barnes et al. (2010). Two models were calculated. First, the total GMV was predicted by group and nuisance variables (Equation 1).

$$\text{Total GMV} \sim \text{Group} + \text{TIV} + \text{Age} + \text{Gender} \quad (1)$$

Second, to analyze the ROIs, a multivariate model was used where the residual correlation between the response variables was assumed (Equation 2).

$$\left(\text{GMV}_{\text{mPFC}}, \text{GMV}_{\text{IFG}}, \text{GMV}_{\text{CN}}, \text{GMV}_{\text{putamen}}\right) \sim \text{Group} + \text{TIV} + \text{Age} + \text{Gender} \quad (2)$$

Further, to investigate whether the medication had affected the GMV of patients, two separate models for only SZ patients were calculated where CPZ was used as a predictor of total GMV (Equation 3) and GMV of targeted ROIs (Equation 4). Notably, it is not possible to use CPZ data in a model that includes both healthy controls and patients, as CPZ data separates two groups perfectly (i.e., CPZ $>$ 0 for all patients except one, and CPZ = 0 for healthy controls), which cause complete collinearity with the factor Group, making the models predictions unreliable.

$$\text{Total GMV}_{\text{Patients}} \sim \text{TIV} + \text{Age} + \text{Gender} + \text{CPZ} \quad (3)$$

$$\left(\text{GMV}_{\text{mPFC}}, \text{GMV}_{\text{IFG}}, \text{GMV}_{\text{CN}}, \text{GMV}_{\text{putamen}}\right) \sim \text{TIV} + \text{Age} + \text{Gender} + \text{CPZ} \quad (4)$$

For analyzing the relationship between cognitive stability and flexibility and the VBM data, accuracy in the switch-drift task was used. Measures of flexibility and stability of predictions were determined based on signal detection theory (Snodgrass & Corwin, 1988). That is, the flexibility of predictions was quantified by the rate of correct detections of switches, i.e., hit rate. In contrast, the stability of predictions was determined by the amount of ignored drifts, i.e., correct rejection (CR) rate. In order to test the relationship between VBM in ROIs and behavioral data, the following BMLM (Equation 5) was employed, where, again, we assumed the residual correlation between the response variables. In this model, we focused on the correlations between behavioral performance and GMV of the selected ROIs. Thus, no additional covariate, such as TIV, age, and gender, was added to the model, as doing so might distort the effects due to multicollinearity between measures. Notably, in the

model, we intentionally did not assume any interaction between CRs and Hits, as these two are theoretically and empirically independent (Trempler et al., 2017). Finally, both groups (i.e., patients and healthy controls) were included in the model to test the group effect after accounting for CRs and Hits.

$$\left(\mathrm{GMV}_{\mathrm{mPFC}}, \mathrm{GMV}_{\mathrm{IFG}}, \mathrm{GMV}_{\mathrm{CN}}, \mathrm{GMV}_{\mathrm{putamen}}\right) \sim \mathrm{CRs} + \mathrm{Hits} + \mathrm{Group} \quad (5)$$

For calculating Bayesian hierarchical generalized linear models, brms (Bürkner, 2017) and RSTan (https://mc-stan.org/) were employed. As all the models were multivariate, uninformative priors were preferred (Bürkner, 2017). Hence, we used $N(0, 10)$ as uninformative priors in the models for β coefficients, $N(0,100)$ for β coefficient of Group when applicable, $\mathrm{student\_t}(3, 0, 2.5)$ for intercepts, $\mathrm{student\_t}(3, 0, 1)$ for sigmas, and $\mathrm{lkj}(1)$ for residual correlations when applicable. All models were calculated with four chains, each having 5000 iterations with 2000 warmups. If any variable showed a *Rhat* (i.e., the potential scale reduction factor on split chains) above 1.05, the model was recalculated with increased iterations and reported accordingly.

All hypotheses were tested using the hypothesis package included in brms (Bürkner, 2017). Based on the suggestion of van Doorn et al. (2021), Bayes factors (BF) > 3 and $BF < \frac{1}{3}$ were considered as significant evidence for accepting and rejecting the tested hypothesis, respectively. One-sided hypotheses (denoted by: BF_{+0} and BF_{-0}) were the comparison of the posterior probability of hypotheses against their alternative; two sided-tests (denoted by: BF_{01}) were the comparison between hypotheses and their alternative computed via the Savage-Dickey density ratio method.

Finally, to check the whole brain data with previous findings (e.g., Antonova et al., 2005; Sigmundsson et al., 2001; Williams, 2008), the Group effect was calculated using general linear models (GLM) embedded in SPM12. In this analysis, TIV was used as a nuisance variable. For finding these anatomical differences, we chose a high primary threshold (i.e., $p < .005$, contigueous voxels > 80), based on the suggestions of Woo et al. (2014), to enhance spatial localization and interpretability. This approach has been discussed to provide the best balance between the type I and II errors in fMRI studies (Lieberman & Cunningham, 2009; Woo et al., 2014).

3 | RESULTS

3.1 | Demographic data

A detailed descriptive summary of the demographics and clinical characteristics of the sample is shown in Table 1. First, we confirmed that SZ patients and the control group were comparable regarding basic demographic data, i.e., age, gender, and handedness. Further, as expected, the two groups differed with respect to SZ symptoms, SAPS, and SANS, as well as in regard to individual history of substance abuse.

3.2 | Gray matter volumetric differences between SZ patients and healthy controls

For the whole brain analysis, the BLM model (Equation 1) converged successfully, with all parameters having

TABLE 1 Demographics and clinical characteristics of the sample population.

Characteristics	Mean (±*SD*)			
	SZ patients ($n = 21$)	Healthy controls ($n = 22$)	Test statistic	*p*-value
Age (years)	35.67 (±9.91)	38.23 (±12.26)	$U = 208.5$	.584
Gender (female/male)	7/14	9/13	$\chi^2 = 0.26$	.607
Handedness (right/left)	19/2	19/3	$\chi^2 = 0.18$	.674
Substance abuse	12 (57.1%)	0	$U = 17.4$	<.001***
CPZ (mg)	639.63 (±427.12)	–	–	–
Illness duration (years)	12.0 (±10.07)	–	–	–
Age of onset (years)	23.5 (±5.40)	–	–	–
SAPS	15.67 (±17.25)	0 (±0)	$U = 396$	<.001***
SANS	20.86 (±17.82)	0.05 (±0.21)	$U = 439$	<.001***

Abbreviations: CPZ, chlorpromazine equivalents; SANS, Scale for the Assessment of Negative Symptoms; SAPS, Scale for the Assessment of Positive Symptoms; SD, standard deviation; SZ, schizophrenia spectrum disorders.

***$p < .001$.

$\hat{R} = 1.0$; further, all parameters were sampled sufficiently, as all tail and bulk effective sample sizes were over 8000. The results of the model clearly showed that total GMV decreases with increasing age (H_-: Age < 0; mean = −2.91 [−3.6, −2.23], $E.E. = 0.42$, $\boldsymbol{p.p.} > .99$, $\boldsymbol{BF_{-0} > 9999}$), and TIV positively predicts total GMV (H_+: TIV > 0; mean = 0.45 [0.39, 0.5], $E.E. = 0.03$, $\boldsymbol{p.p.} > .99$, $\boldsymbol{BF_{+0} > 9999}$) Gender, however, did not significantly affect total GMV (H_0: Gender = 0; mean = 4.03 [−10.67, 18.52], $E.E. = 7.52$, $p.p. = .54$, $BF_{01} = 1.18$). Finally, as expected, total GMV was significantly lower in patients with SZ compared to healthy controls (H_-: Group < 0; mean = −26 [−40.94, −11.06], $E.E. = 9.12$, $\boldsymbol{p.p.} > .99$, $\boldsymbol{BF_{-0} = 341.86}$).

Additionally, to confirm that patients' medication usage is not a confound in the previous model, a BLM for patients only (Equation 3) was calculated to measure the effects of CPZ on whole brain GMV. Notably, the results showed strong evidence that CPZ did not affect GMV (H_0: CPZ = 0; mean = 0.45 [0.39, 0.5], $E.E. = 0.03$, $\boldsymbol{p.p.} > .99$, $\boldsymbol{BF_{+0} > 9999}$ **405.74**). Further, the results showed the same pattern as the previous model regarding TIV (H_+: TIV > 0; mean = 0.41 [0.33, 0.49], $E.E. = 0.05$, $\boldsymbol{p.p.} > .99$, $\boldsymbol{BF_{+0} > 9999}$), age ($H_-$: Age < 0; mean = −3.38 [−4.69, −2.06], $E.E. = 0.8$, $\boldsymbol{p.p.} > .99$, $\boldsymbol{BF_{-0} = 5999}$), and gender ($H_0$: Gender = 0; mean = 2.66 [−15.19, 19.99], $E.E. = 8.82$, $p.p. = .52$, $BF_{01} = 1.08$).

Further, to compare our whole brain results with previous findings, a GLM was calculated via SPM12. The results are shown in Figure 2, and the list of all brain areas that showed significant atrophy in SZ patients compared to healthy controls is presented in Table A1.

Afterward, we focused on the a-priori-defined anatomical ROIs. The VBM results were modeled using BMLM, which converged successfully with all parameters having $\hat{R} = 1.0$. For the ROI model (Equation 2), similar to the whole brain model, all parameters were sampled sufficiently, as indicated by tail and bulk effective sample sizes over 8000. The parameter estimations and hypotheses tests for all responses (i.e., different ROIs) are presented in Table 2. The results of BMLM clearly showed that the GVM in mPFC, IFG, and CN were significantly smaller for SZ patients compared to healthy controls (Figure 3). For putamen, however, there was weak evidence to reject our hypothesis (Group <0), meaning one might assume that GMV in putamen is not decreased due to SZ disease (Figure 3).

Further, the results (Table 2) indicate that (I) GMVs decreased with increasing age in all ROIs, (II) as TIV increased, the GMVs of all ROIs were significantly increased, and finally, (III) there was substantial evidence corroborating the null hypotheses regarding gender in all ROIs, meaning that gender did not affect GMVs in any of the selected ROIs.

Critically, the patient-only BMLM (Equation 4) showed strong evidence that medication does not predict the GMV in any of the a-priori-defined ROIs. The rest of the findings regarding TIV, age, and gender are similar to the full BLML (Equation 2) discussed above, which includes both healthy controls and patients (for the full results of the patient-only model, see Table A2).

3.3 | Structural correlates of flexibility and stability of predictions in SZ patients

To understand the structural correlates of cognitive stability and flexibility, we used BMLM (Equation 5), where GMVs in selected ROIs were predicted via behavioral performance in the switch-drift task for both healthy controls and SZ patients. The behavioral results are based on the calculations of Standke et al. (2021) and, therefore, are not reported here anew. The results showed that hit rates, indicating flexible shifts in predictions, were positively correlated with GMV in mPFC (H_0: Hits = 0; mean = 7.87 [3.53, 12.24], $E.E. = 2.23$, $\boldsymbol{p.p.} = .02$, $\boldsymbol{BF_{01} = 0.02}$; Figure 4a), IFG ($H_0$: Hits = 0; mean = 3.48 [1.26, 5.69], $E.E. = 1.13$, $p.p. = .09$, $\boldsymbol{BF_{01} = 0.1}$; Figure 4b), and CN ($H_0$: Hits = 0; mean = 0.81 [0.37, 1.26], $E.E. = 0.23$, $p.p. = .12$, $\boldsymbol{BF_{01} = 0.13}$; Figure 4c**)**. However, substantial evidence supported the null hypothesis concerning the putamen (H_0: Hits = 0; mean = 0.67 [−0.01, 1.35], $E.E. = 0.34$, $p.p. = .81$, $\boldsymbol{BF_{01} = 4.26}$; Figure 4d).

Regarding correct rejections (CR), which are considered to be related to the stability of generative predictions, the model (Equation 5) results indicated substantial evidence supporting the null hypothesis for the IFG (H_0: CR = 0; mean = 1.31 [−2.81, 5.46], $E.E. = 2.1$, $p.p. = .79.$, $\boldsymbol{BF_{01} = 3.86}$), the CN ($H_0$: CR = 0; mean = 0.08 [−0.78, 0.95], $E.E. = 0.43$, $\boldsymbol{p.p.} = .96$, $\boldsymbol{BF_{01} = 22.54}$), and putamen ($H_0$: CR = 0; mean = 0.12 [−1.21, 1.45], $E.E. = 0.68$, $p.p. = .94$, $\boldsymbol{BF_{01} = 15.25}$**)**, and further, did not support or reject the null hypothesis concerning the mPFC (H_0: CR = 0; mean = 1.4 [−6.79, 9.57], $E.E. = 4.15$, $p.p. = .071$, $BF_{01} = 2.4$).

Finally, the group differences in regional GMV were eliminated after considering the effects of correct rule switch detections and correct rejections of drifts, which is observable in substantial evidence for accepting the null hypothesis regarding group differences (i.e., H_0: Group = 0) after correcting for behavioral outcomes in all of the ROIs: mPFC (H_0: Group = 0; mean = 1.31 [−0.7, 3.33], $E.E. = 1.02$, $\boldsymbol{p.p.} = .98$, $\boldsymbol{BF_{01} = 41.7}$), IFG ($H_0$: Group = 0; mean = 0.69 [−0.33, 1.7], $E.E. = 0.51$, $\boldsymbol{p.p.} = .99$, $\boldsymbol{BF_{01} = 72.6}$), the CN ($H_0$: Group = 0; mean = 0.13 [−0.07, 0.33], $E.E. = 0.1$, $\boldsymbol{p.p.} > .999$, $\boldsymbol{BF_{01} = 449.11}$**)**, and the putamen ($H_0$: Group = 0; mean = 0.29 [−0.02, 0.6], $E.E. = 0.16$, $\boldsymbol{p.p.} = .99$, $\boldsymbol{BF_{01} = 110.82}$).

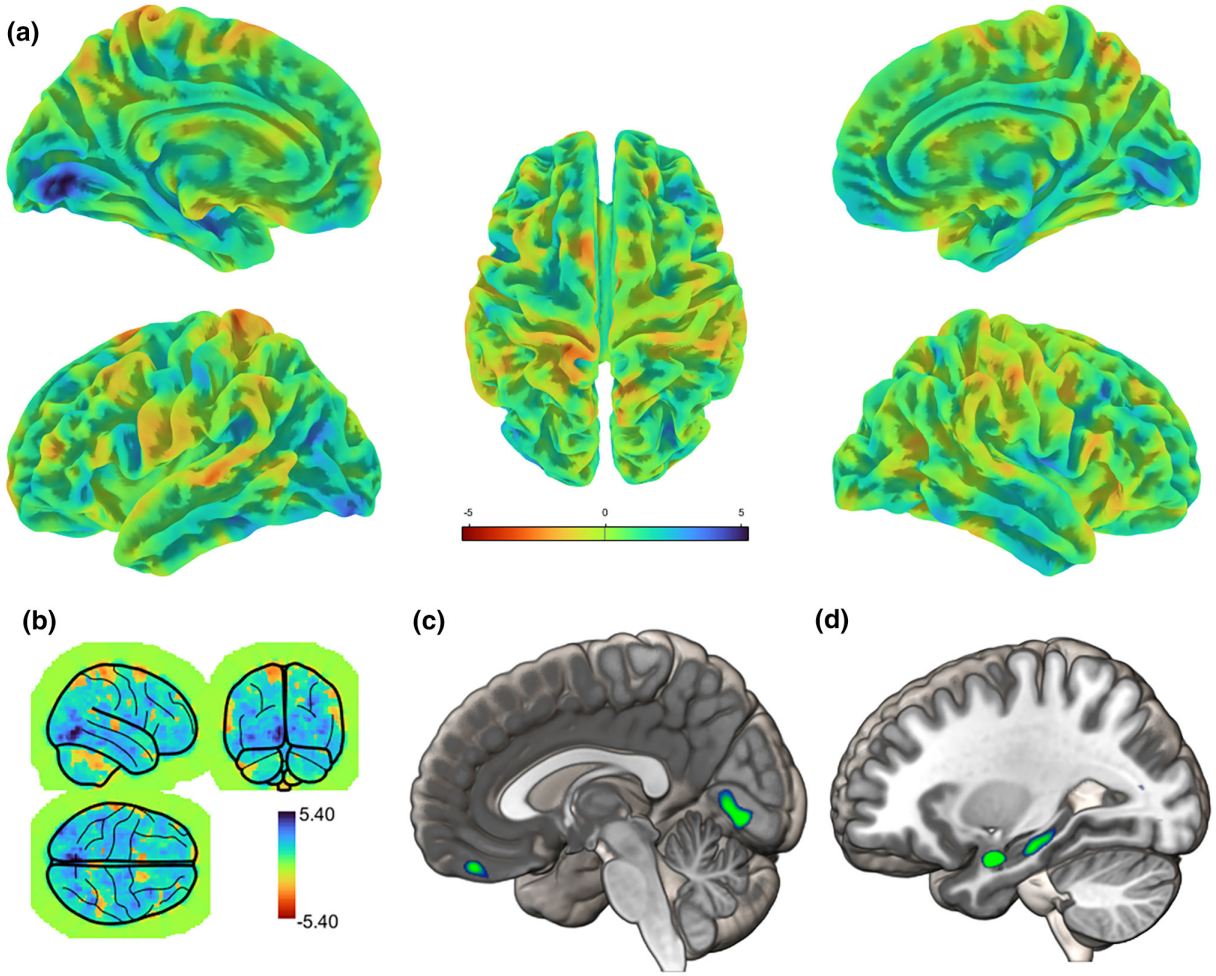

FIGURE 2 The *t*-map of the gray matter volume (GMV) differences between schizophrenia spectrum patients (SZ) and healthy controls. The (a) volume and (b) surface maps were generated using the CAT12 toolbox (Gaser & Kurth, 2020) and corrected for total intracranial volume differences (TIV). Negative and positive values show a reduction (the blue spectrum) and increase (the red spectrum) in GMV in SZ patients compared to healthy controls, respectively. (c and d) The sagittal brain cuts depicting some of the brain areas that showed significant atrophy in SZ patients compared to healthy controls in the whole brain analysis with $p < .005$ and $k > 80$. The highlighted areas are the lingual gyrus (c), the orbitofrontal cortex (c), the amygdala extending into the hippocampus proper (d), and the posterior hippocampus (d). For the entire list and Montreal Neurologic Institute (MNI) coordinates of significant differences between SZ patients and healthy controls, see Table A1.

Together, our results suggest that cognitive flexibility is related to gray matter atrophy in the mPFC, IFG, and CN, whereas cognitive stability did not rely on the structural integrity of these targeted anatomical structures in our sample. Additionally, the putamen was not involved in stabilizing or incorporating flexible shifts in generative predictions. Furthermore, the differences in GMVs between the two groups were fully explained when one considered the effects of behavioral task outcomes (i.e., hit rates and correct rejections), indicating that GMV losses in the selected ROIs are critically involved in the pathological deficiencies of SZ regarding cognitive flexibility and stability.

4 | DISCUSSION

Previous studies revealed that diminished cognitive stability and flexibility in SZ patients could be attributed to functional abnormalities in frontostriatal circuits (Cadena et al., 2018, 2019; Standke et al., 2021), in particular to the striatum and frontal areas, i.e., mPFC and IFG (Standke et al., 2021). The overarching aim of the present study was to investigate the relationships between the structural integrity of anatomical brain areas within frontostriatal networks, highlighted based on our previous results (Standke et al., 2021), and deficient cognitive stability and flexibility in patients with SZ compared to healthy controls. As

TABLE 2 Voxel-based morphometry results of a-priori-defined anatomical ROIs.

Response	Coefficient	Estimate [95% C.I.]	*E.E.*	Hypothesis	*p.p.*	*B.F.*
mPFC	Group	−1.06 [−1.74, −0.39]	0.41	Group <0	**>.999**	**229.77**
	TIV	0.02 [0.01, 0.02]	0.0017	TIV>0	**>.999**	**>9999**
	Age	−0.14 [−0.17, −0.1]	0.02	Age<0	**>.999**	**>9999**
	Gender	−0.44 [−1.45, 0.59]	0.52	Gender=0	.93	**13.18**
IFG	Group	−0.42 [−0.91, 0.06]	0.29	Group <0	.93	**12.73**
	TIV	0.01 [0.005, 0.036]	0.001	TIV>0	**>.999**	**5999**
	Age	−0.07 [−0.09, −0.05]	0.01	Age<0	**>.999**	**>9999**
	Gender	0.16 [−0.56, 0.9]	0.37	Gender=0	**.96**	**24.77**
CN	Group	−0.12 [−0.22, −0.02]	0.06	Group <0	**.98**	**45.51**
	TIV	0.001 [0.0008, 0.0017]	0.0003	TIV>0	**>.999**	**>9999**
	Age	−0.01 [−0.02, −0.01]	0.002	Age<0	**>.999**	**>9999**
	Gender	0.05 [−0.1, 0.2]	0.08	Gender=0	**.99**	**112.23**
Putamen	Group	0.06 [−0.1, 0.22]	0.1	Group <0	.28	0.38
	TIV	0.001 [0.004, 0.001]	0.0004	TIV>0	**.995**	**243.898**
	Age	−0.01 [−0.02, −0.01]	0.004	Age<0	**>.999**	**1332.33**
	Gender	0.22 [−0.02, 0.47]	0.12	Gender=0	.94	**15.28**

Note: Highlighted Bayes factor and posterior probabilities show at least substantial evidence supporting the tested hypothesis (van Doorn et al., 2021).

Abbreviations: B.F., Bayes Factor; C.I., credential interval; CN, caudate nucleus; E.E., estimation error; IFG, inferior frontal gyrus; mPFC, medial prefrontal cortex; p.p., posterior probability; SZ, schizophrenia spectrum disorder.

suggested by previous meta-analyses (Gupta et al., 2015; Haijma et al., 2013; Williams, 2008), our results showed that total GMV was decreased in SZ patients compared to healthy participants. Further, we found GMVs in a-priori-defined ROIs within the frontostriatal network, i.e., mPFC, IFG, and the CN, to be decreased in SZ patients compared to healthy controls. Notably, GMVs of these regions (mPFC, IFG, and the CN) predicted the ability of patients and healthy controls to detect switches of the prediction rule but not their ability to ignore prediction drifts without rule changes, indicating a critical role of the structural integrity of these regions in the flexibility, but not stability, of generative models, regardless of the SZ disease.

In the current study, we found that the GMV of the mPFC was significantly reduced, which is in line with previous research (Bonilha et al., 2008; Gupta et al., 2015; Shepherd et al., 2012; Sigmundsson et al., 2001; Williams, 2008; Zhang et al., 2018). Compelling evidence for the notion of medial prefrontal pathology in SZ comes from studies (e.g., Pomarol-Clotet et al., 2010) integrating multiple imaging methods, such as VBM, functional MRI, and diffusion tensor imaging (DTI). The results of these studies (e.g., Pomarol-Clotet et al., 2010) indicate that reduced mPFC GMV is associated with abnormal activation patterns and altered structural connectivity of the mPFC in SZ patients, corroborating the notion that the mPFC is structurally and functionally abnormal in SZ. Beyond structural abnormalities of mPFC in SZ patients, our results show that cognitive flexibility depends on the structural integrity of the mPFC, which perfectly aligns with our previous findings showing that attenuated mPFC functional activity was related to inflexibility in SZ patients (Standke et al., 2021) and healthy participants (Trempler et al., 2017) using the fMRI data of the same population investigated here. In fact, out of all investigated ROIs, the mPFC showed the strongest association with flexible updating of predictions. The role of the mPFC in cognitive flexibility is well-recognized (Klune et al., 2021). Several studies found that increased mPFC activity is associated with flexible updating (e.g., Armbruster et al., 2012; Wang et al., 2017), set-switching (Floresco et al., 2009; Wilmsmeier et al., 2010), and initiating behavioral adaptation in response to prediction errors (Egner, 2011). Considering previous findings and our results, one can conclude that compromised structural integrity of the mPFC might underlie deficient cognitive flexibility in SZ patients.

Regarding the IFG, our results showed (I) significant GMV reduction in SZ patients compared to healthy controls, which is in line with previous research (Antonova et al., 2005; Dietsche et al., 2017; Gupta et al., 2015; Sigmundsson et al., 2001; Williams, 2008). Further, our results showed (II) a relationship between the structural integrity of the IFG and cognitive flexibility but not stability. This finding, however, contrasts with previous studies showing the involvement of the IFG in stabilizing predictive models (Trempler et al., 2017), corroborating its role

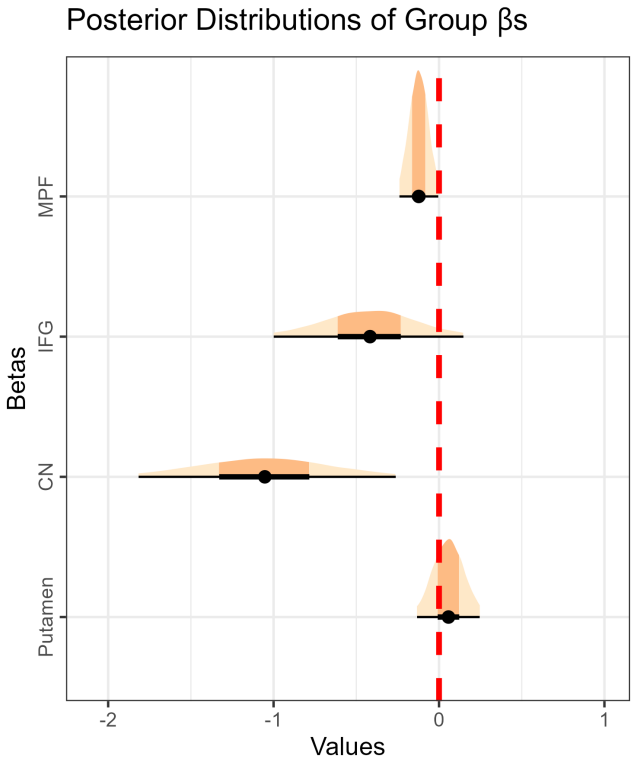

FIGURE 3 Modeling of gray matter volumes (GMVs) in different regions of interest (ROIs). Density plots of posterior distributions of Group β-coefficients included in the ROI model (Equation 2). Orange and yellow shadows represent the 50% and 95% highest probability density (HPD) areas, respectively. When HPD does not include zero (represented with the red dashed line), the evidence supports with a 95% credential interval that the coefficient is significant in the model. However, as using arbitrary posterior probability (p.p.) for significance checking is criticized (Dienes, 2016), we additionally used the Bayes factor to evaluate each coefficient's contribution to the model (Table 2). CN, caudate nucleus; IFG, inferior frontal gyrus; MPF, medial prefrontal cortex.

in response inhibition (e.g., Aron et al., 2014; Chambers et al., 2007; Schaum et al., 2021) and distracter resistance (Wager et al., 2014). Specifically, the impairment in ignoring drift events was found to correlate with a significant increase in right IFG volume in patients with Parkinson's disease (Trempler et al., 2018). However, one should consider that these findings stem from studies in Parkinson's disease patients and may not readily generalize to SZ. Moreover, the right IFG showed stronger activity for drifts than switches in healthy young subjects (Trempler et al., 2017). Further, the fMRI results of the same population (Standke et al., 2021) showed that activity in the IFG is associated with cognitive stability in patients with SZ. It is vital to consider that this area has been reported to be reduced in volume by other researchers (Dietsche et al., 2017; Williams, 2008), and therefore, we selected IFG as an ROI for drift-related deficits. However, although SZ patients in our sample showed behavior deficits in ignoring drifts, and we also observed a reduction in IFG GMV, our results supported the null hypothesis regarding the correlation between IFG and correct rejections. In the current study, our IFG-ROI was averaged over both hemispheres, which contrasts with some previous studies (e.g., Antonova et al., 2005; Trempler et al., 2018). Nevertheless, when we used right and left IFG as our ROIs as well, the results did not change (for detailed results, see Table A3). Therefore, it is conceivable that cognitive stability is primarily associated with the structural integrity of subregions of IFG that are not necessarily aligned with anatomical segregations. Another reason why we did not find any association between GMV in different ROIs and the ability to shield against distracters is the fact that the current task design prevents dissociating between not responding and shielding against distractors (Standke et al., 2021). Accordingly, as SZ patients, compared to healthy controls, are more prone to not respond to the employed task (Standke et al., 2021), the correct rejections are then a measure of mental stability and inclination to respond simultaneously. Therefore, future studies should replicate our results using designs that can distinguish between not responding and shielding against distractors before one can draw firm conclusions.

The IFG might be engaged in both flexibility and stability to at least some extent. In fact, several previous studies (e.g., Armbruster et al., 2012; Kim et al., 2011) revealed that inferior frontal areas contribute to cognitive flexibility. Armbruster et al. (2012) argue that this might be because updating internal models depends on several cognitive operations, including the inhibition of the old model. Fittingly, a conjunction of switch and drift events revealed significant engagement of the right IFG (Trempler et al., 2020). Also, SZ patients, compared to healthy controls, showed decreased activity of the opercular part of the right IFG (BA 44) for switches but decreased activity of the orbital part of the right IFG (BA 47) for drifts (Standke et al., 2021). Accordingly, different subregions of the IFG could be differently affected by atrophy in SZ, resulting in mixed findings depending on the investigated sample. In sum, further studies are needed to understand the role of the right IFG and its subregions in cognitive flexibility and stability in SZ. Nonetheless, the present results corroborate the notion of tightly interconnected frontostriatal networks supporting cognitive flexibility, thereby adding to existing evidence that suggests highly interconnected medial and lateral prefrontal areas working cooperatively to facilitate responses when encountering prediction errors (Alexander & Brown, 2011).

In line with previous results (e.g., Ebdrup et al., 2010), we found GMV in the CN, but not in the putamen, to be significantly diminished in SZ patients compared

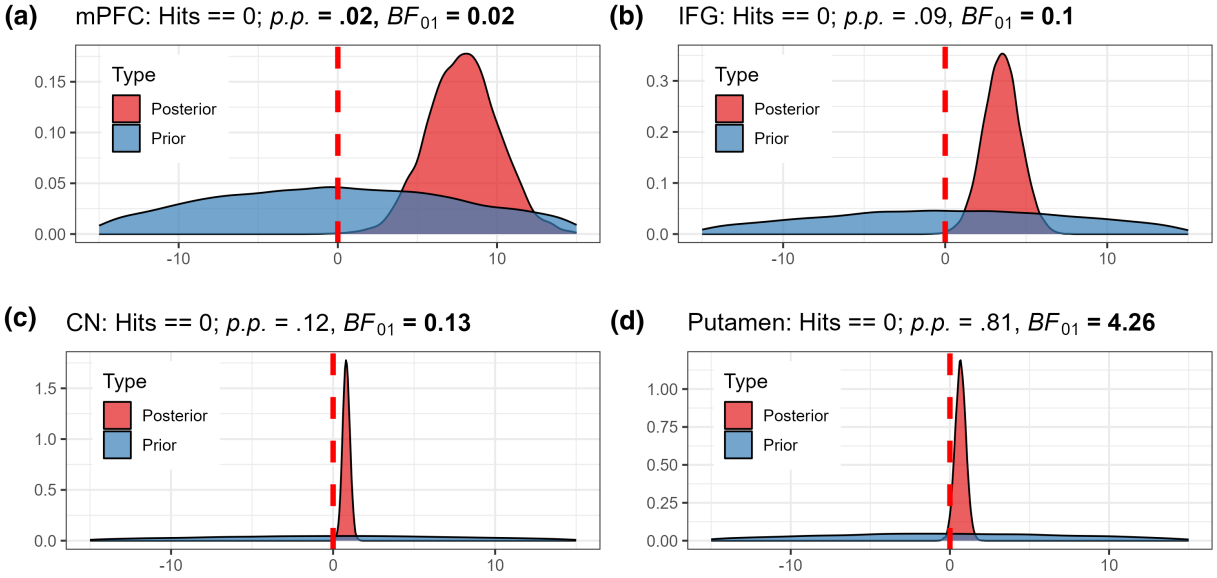

FIGURE 4 Modeling of gray matter volumes (GMVs) in different ROIs (a–d). The posterior and prior distributions testing hypotheses regarding the correlation between Hits and GMVs in different anatomical a-priori-defined ROIs. The distributions are extracted from the BMLM correlation model (Equation 5). The Savage-Dickey density ratio method was used for two-sided (point) hypothesis testing. The presented Bayes factor is the evidence ratio between the hypothesis and its alternative, i.e., the posterior density at the point of interest divided by the prior density at that point. Values greater than one indicate that the evidence favors the point hypothesis (Bürkner, 2017). As the two-sided hypotheses tested here are the null hypothesis, the point (zero) is shown by red dashed lines.

to controls. This volume reduction in the CN is further corroborated by cellular postmortem studies (e.g., Kreczmanski et al., 2007) that found that the number of neurons in the CN of SZ patients is reduced by 10%. Additionally, the present result corresponds well with studies reporting a profound progressive caudate gray matter loss associated with SZ (Dietsche et al., 2017; van Haren et al., 2007). Moreover, we tested whether caudate volume reduction relates to deficiency in responding to prediction errors, i.e., detection of switches and shielding of distracters. Indeed, we found that diminished accuracy in detecting rule shifts, but not ignoring drifts, is correlated with a lower volume of the CN. Accordingly, the behavioral effects regarding switch detection and ignoring drifts fully explained the difference between SZ patients and healthy controls in caudate volume. The present observation aligns well with findings that associate the CN with flexible behavior adaptation, enabling goal-directed actions (Grahn et al., 2008). The CN was shown to code for breaches of expectancy during movement observation. Importantly, the CN activity could not be explained by the increased saliency-triggered attention or the requirement to change ongoing behavior in response to the surprising event (Schiffer & Schubotz, 2011). In line with this view, in our previous studies using the present paradigm, we found that caudate activity was related to discrimination efficiency when encountering switches or drifts (i.e., the proportion of hits minus the proportion of false alarms) in both healthy subjects and patients with SZ (Standke et al., 2021; Trempler et al., 2017). Moreover, reduced signaling of the caudate in Parkinson's disease patients who were off medication correlated with a deficiency in adapting to the increasing probability of switches and ignoring highly surprising drifts (Trempler et al., 2020). These previous findings might show that specific behavioral implications of both event types are implemented at this processing stage. Extending our previous findings suggesting impaired modulation of correct response selection due to impaired caudate signaling (Standke et al., 2021), the present results further suggest an association between structural abnormalities of the CN and behavioral measures of flexibility in SZ. However, we did not find any association between caudate volume and impaired cognitive stability in SZ. Since cognitive stability arguably requires fewer cognitive resources than cognitive flexibility (Armbruster et al., 2012), it is conceivable that cognitive stability is less susceptible to structural pathology of the striatum, and therefore, no relationship was found with the rate of drift rejections. However, as discussed for IFG, the measure of cognitive stability in the current experiment (Standke et al., 2021) does not allow for firm conclusions since proneness to not responding cannot be dissociated from cognitive stability.

Interestingly, contrary to the CN, we did not find any association between GMV in the putamen and cognitive flexibility or stability. The former is known to connect

to higher-order associative areas such as the mPFC or IFG (i.e., association loop), whereas the putamen is connected to sensorimotor areas (i.e., motor loop) (Alexander et al., 1986). Correspondingly, the CN is involved in higher cognitive (i.e., executive) functioning (Grahn et al., 2008), thus constituting a potentially crucial etiological factor for cognitive impairment in SZ (Simpson et al., 2010). In other words, our results regarding the putamen and CN might indicate that deficient cognitive flexibility in patients with SZ is associated with alterations in the association rather than the motor loop, contrary to what is found for patients with Parkinson's (Trempler et al., 2020).

Our whole-brain analysis results showed in SZ patients, compared to healthy controls, several regions showed significant atrophy; intriguingly, these brain areas were closely related to previous findings (e.g., Antonova et al., 2005; Sigmundsson et al., 2001; Williams, 2008). For instance, similar to our results, several other studies found a reduction in the lingual gyrus (e.g., Antonova et al., 2005), the hippocampus (for review, see Williams, 2008), and the orbitofrontal cortex (e.g., Hulshoff Pol et al., 2004; Sigmundsson et al., 2001). Based on these results, one might cautiously suggest that our findings are generalizable to other samples of SZ patients.

Finally, in our models considering the associations between GMV in ROIs and behavioral performance, we found that the group differences (i.e., healthy controls vs. SZ patients) were resolved when one considers the behavioral outcomes. These results are aligned with the previous findings showing that SZ patients and healthy controls use the same networks for responding to the demands of cognitive tasks (Meram et al., 2023; Oliver et al., 2021; Sheffield et al., 2015). Our results extend these findings by showing that although SZ patients and healthy controls might use the same regions for responding to cognitive demands, anatomical atrophies in these areas will lead to worse performance in SZ patients.

Several limitations of the current study should be acknowledged here. First, the present study focused on relationships between structural differences between SZ patients and healthy controls, and therefore, we recruited patients with different disorders within the schizophrenia spectrum. The results, although generalizable, cannot inform about the relationship between different subcategories and observed structural changes. Future studies should focus on the disease type as a factor of interest now that the basic relationships are clarified.

Second, the current results cannot address whether volumetric brain reductions cause deficient stability and flexibility of prediction or are the results of other pathological developments and, therefore, correlated with cognitive symptoms. Especially as volumetric analyses do not provide information about the exact underlying pathology reflected by volume loss (Walterfang et al., 2006), one should be cautious when interpreting the current results. One should especially consider that the maturation of the frontostriatal areas is comparably long, extending well into adolescence and early adulthood, which overlaps with SZ onset (Klune et al., 2021). Therefore, longer maturation periods of frontostriatal areas make them prone to neurodevelopmental pathology in SZ, which might explain both cognitive deficiencies and structural abnormalities observed in the current study. However, in order to address such questions, it is necessary to conduct longitudinal studies, which is out of the scope of the present study.

Third, the sample size of the current study, even though comparable to some other studies (e.g., Meram et al., 2023), is generally considered small. However, the current study uses Bayesian statistics to provide statistical insights regardless of the sample size (Dienes, 2016; Dienes & McLatchie, 2018). Specifically, as we found substantial evidence using non-informative priors (Scott & Berger, 2006), the current results substantially contribute to the field. However, it is important to note that the current sample cannot predict effects in a sample with different characteristics regardless of the statistical methods used. In other words, changing sample characteristics might change the results. For instance, in the current sample, we had a predominantly male patient group. Therefore, the results regarding gender differences should be taken cautiously, as we had only seven female patients, which might limit the generalizability of the current study regarding gender similarities in regard to GMV losses.

Fourth, the switch-drift task used in the current study (Trempler et al., 2017, 2018) was better in measuring cognitive flexibility rather than stability. Since cognitive stability was related to response inhibition in the employed task, the tendency to not respond (Snodgrass & Corwin, 1988) could not be fully separated from cognitive stability (Standke et al., 2021). Hence, in future studies, it is vital to expand and replicate the current results regarding cognitive stability with a task that requires a response for measuring both cognitive stability and flexibility.

Another point regarding the current study is the choice of ROIs. Although the selection of anatomical ROIs in the current study was theoretically driven and based on the previous studies that focused on cognitive stability and flexibility (e.g., Armbruster et al., 2012; Chatham & Badre, 2015; Diederen & Fletcher, 2021; Wang et al., 2017), the choice of ROIs is not unique. Therefore, future studies using different theoretical backgrounds might focus on a different set of ROIs to investigate the

stability and flexibility of cognitive functions. Although we also reported the whole brain analysis to counteract our selection biases for future meta-analyses, the selection criteria should be considered when interpreting the current results.

5 | CONCLUSION

Together, the present study provides stark evidence that SZ-related structural abnormalities in frontostriatal networks underlie deficient cognitive flexibility in these patients. Notably, our results revealed that gray matter atrophy in areas involved in the association loop (i.e., mPFC, IFG, and the CN), rather than the putamen-mediated motor loop, is critically related to the capability of flexibly shifting generative models. Further, significant GMV differences are statistically explainable when one considers the behavioral performance in a switch-drift task, measuring cognitive flexibility and stability. The current results, combined with previous findings, indicate that both morphological and functional abnormalities in frontostriatal networks seem to underlie disrupted striatal gating and prefrontal processing of prediction errors, leading to deficient flexibility of prediction in patients with SZ. Consequently, our results indicate the necessity of developing treatment options to minimize neurodevelopmental and progressive brain atrophy in SZ patients.

AUTHOR CONTRIBUTIONS

Anoushiravan Zahedi: Formal analysis; methodology; validation; visualization; writing – original draft; writing – review and editing. **Florentine Herkströter:** Formal analysis; writing – original draft; writing – review and editing. **Isabel Standke:** Data curation; investigation. **Udo Dannlowski:** Conceptualization; funding acquisition; investigation. **Rebekka Lencer:** Conceptualization; funding acquisition; investigation. **Ricarda I. Schubotz:** Conceptualization; funding acquisition; project administration; supervision; writing – original draft; writing – review and editing. **Ima Trempler:** Conceptualization; data curation; investigation; supervision; writing – original draft; writing – review and editing.

ACKNOWLEDGMENTS

Open Access funding enabled and organized by Projekt DEAL.

FUNDING INFORMATION

This work was supported by intramural funding from the Medical Faculty of the University of Muenster as a personal grant to I.S. The German Research Foundation (DFG, grant FOR2107 DA1151/5-1 and DA1151/5-2 to UD; SFB-TRR58, Projects C09 and Z02 to UD) and the Interdisciplinary Center for Clinical Research (IZKF) of the Medical Faculty of the University of Muenster (grant Dan3/012/17 to UD) supported this work by providing reimbursement for participants.

CONFLICT OF INTEREST STATEMENT

The authors have no relevant financial or non-financial interests to disclose.

DATA AVAILABILITY STATEMENT

The data and models supporting the results of this study are available in a public repository: doi: 10.17605/OSF.IO/C3GKZ.

ETHICS STATEMENT

The study procedures followed the Helsinki Declaration and were approved by the local ethics committee of the University of Muenster. Written informed consent was obtained from participants included in the study.

ORCID

Anoushiravan Zahedi https://orcid.org/0000-0002-5532-3910

REFERENCES

Alexander, G. E., DeLong, M. R., & Strick, P. L. (1986). Parallel organization of functionally segregated circuits linking basal ganglia and cortex. *Annual Review of Neuroscience*, *9*, 357–381. https://doi.org/10.1146/annurev.ne.09.030186.002041

Alexander, W. H., & Brown, J. W. (2011). Medial prefrontal cortex as an action-outcome predictor. *Nature Neuroscience*, *14*(10), 1338–1344. https://doi.org/10.1038/nn.2921

American Psychological Association. (1994). *Diagnostic and statistical manual of mental disorders*. American Psychiatric Press.

Andreasen, N. C. (1984). *The scale for the assessment of positive symptoms (SAPS)*. University of Iowa.

Andreasen, N. C., & Olsen, S. (1982). Negative v positive schizophrenia. Definition and validation. *Archives of General Psychiatry*, *39*(7), 789–794. https://doi.org/10.1001/archpsyc.1982.04290070025006

Andreasen, N. C., Pressler, M., Nopoulos, P., Miller, D., & Ho, B. C. (2010). Antipsychotic dose equivalents and dose-years: A standardized method for comparing exposure to different drugs. *Biological Psychiatry*, *67*(3), 255–262. https://doi.org/10.1016/j.biopsych.2009.08.040

Antonova, E., Kumari, V., Morris, R., Halari, R., Anilkumar, A., Mehrotra, R., & Sharma, T. (2005). The relationship of structural alterations to cognitive deficits in schizophrenia: A voxel-based morphometry study. *Biological Psychiatry*, *58*(6), 457–467. https://doi.org/10.1016/j.biopsych.2005.04.036

Armbruster, D. J., Ueltzhoffer, K., Basten, U., & Fiebach, C. J. (2012). Prefrontal cortical mechanisms underlying individual differences in cognitive flexibility and stability. *Journal of Cognitive Neuroscience*, *24*(12), 2385–2399. https://doi.org/10.1162/jocn_a_00286

Aron, A. R., Robbins, T. W., & Poldrack, R. A. (2014). Inhibition and the right inferior frontal cortex: One decade on. *Trends in Cognitive Sciences*, *18*(4), 177–185. https://doi.org/10.1016/j.tics.2013.12.003

Barnes, J., Ridgway, G. R., Bartlett, J., Henley, S. M., Lehmann, M., Hobbs, N., Clarkson, M. J., MacManus, D. G., Ourselin, S., & Fox, N. C. (2010). Head size, age and gender adjustment in MRI studies: A necessary nuisance? *NeuroImage*, *53*(4), 1244–1255. https://doi.org/10.1016/j.neuroimage.2010.06.025

Beck, A. T., Steer, R. A., & Brown, G. (1996). *Beck depression inventory–II*. APA PsycTests. https://doi.org/10.1037/t00742-000

Bilder, R. M., Volavka, J., Lachman, H. M., & Grace, A. A. (2004). The catechol-O-methyltransferase polymorphism: Relations to the tonic-phasic dopamine hypothesis and neuropsychiatric phenotypes. *Neuropsychopharmacology*, *29*(11), 1943–1961. https://doi.org/10.1038/sj.npp.1300542

Bonilha, L., Molnar, C., Horner, M. D., Anderson, B., Forster, L., George, M. S., & Nahas, Z. (2008). Neurocognitive deficits and prefrontal cortical atrophy in patients with schizophrenia. *Schizophrenia Research*, *101*(1–3), 142–151. https://doi.org/10.1016/j.schres.2007.11.023

Bowie, C. R., & Harvey, P. D. (2005). Cognition in schizophrenia: Impairments, determinants, and functional importance. *The Psychiatric Clinics of North America*, *28*(3), 613-633, 626. https://doi.org/10.1016/j.psc.2005.05.004

Braver, T. S., Barch, D. M., & Cohen, J. D. (1999). Cognition and control in schizophrenia: A computational model of dopamine and prefrontal function. *Biological Psychiatry*, *46*(3), 312–328. https://doi.org/10.1016/s0006-3223(99)00116-x

Bürkner, P.-C. (2017). Brms: An R package for Bayesian multilevel models using Stan. *Journal of Statistical Software*, *80*(1), 1–28. https://doi.org/10.18637/jss.v080.i01

Cadena, E. J., White, D. M., Kraguljac, N. V., Reid, M. A., Jindal, R., Pixley, R. M., & Lahti, A. C. (2019). Cognitive control network dysconnectivity and response to antipsychotic treatment in schizophrenia. *Schizophrenia Research*, *204*, 262–270. https://doi.org/10.1016/j.schres.2018.07.045

Cadena, E. J., White, D. M., Kraguljac, N. V., Reid, M. A., & Lahti, A. C. (2018). Evaluation of fronto-striatal networks during cognitive control in unmedicated patients with schizophrenia and the effect of antipsychotic medication. *NPJ Schizophrenia*, *4*(1), 8. https://doi.org/10.1038/s41537-018-0051-y

Chambers, C. D., Bellgrove, M. A., Gould, I. C., English, T., Garavan, H., McNaught, E., Kamke, M., & Mattingley, J. B. (2007). Dissociable mechanisms of cognitive control in prefrontal and premotor cortex. *Journal of Neurophysiology*, *98*(6), 3638–3647. https://doi.org/10.1152/jn.00685.2007

Chatham, C. H., & Badre, D. (2015). Multiple gates on working memory. *Current Opinion in Behavioral Sciences*, *1*, 23–31. https://doi.org/10.1016/j.cobeha.2014.08.001

Diederen, K. M. J., & Fletcher, P. C. (2021). Dopamine, prediction error and beyond. *The Neuroscientist*, *27*(1), 30–46. https://doi.org/10.1177/1073858420907591

Dienes, Z. (2016). How Bayes factors change scientific practice. *Journal of Mathematical Psychology*, *72*, 78–89. https://doi.org/10.1016/j.jmp.2015.10.003

Dienes, Z., & McLatchie, N. (2018). Four reasons to prefer Bayesian analyses over significance testing. *Psychonomic Bulletin & Review*, *25*(1), 207–218. https://doi.org/10.3758/s13423-017-1266-z

Dietsche, B., Kircher, T., & Falkenberg, I. (2017). Structural brain changes in schizophrenia at different stages of the illness: A selective review of longitudinal magnetic resonance imaging studies. *The Australian and New Zealand Journal of Psychiatry*, *51*(5), 500–508. https://doi.org/10.1177/0004867417699473

Ebdrup, B. H., Glenthoj, B., Rasmussen, H., Aggernaes, B., Langkilde, A. R., Paulson, O. B., Lublin, H., Skimminge, A., & Baare, W. (2010). Hippocampal and caudate volume reductions in antipsychotic-naive first-episode schizophrenia. *Journal of Psychiatry & Neuroscience*, *35*(2), 95–104. https://doi.org/10.1503/jpn.090049

Egner, T. (2011). Surprise! A unifying model of dorsal anterior cingulate function? *Nature Neuroscience*, *14*(10), 1219–1220. https://doi.org/10.1038/nn.2932

Floresco, S. B., Zhang, Y., & Enomoto, T. (2009). Neural circuits subserving behavioral flexibility and their relevance to schizophrenia. *Behavioural Brain Research*, *204*(2), 396–409. https://doi.org/10.1016/j.bbr.2008.12.001

Frank, M. J., Loughry, B., & O'Reilly, R. C. (2001). Interactions between frontal cortex and basal ganglia in working memory: A computational model. *Cognitive, Affective, & Behavioral Neuroscience*, *1*(2), 137–160. https://doi.org/10.3758/cabn.1.2.137

Gaser, C., Dahnke, R., Kurth, K., Luders, E., & Alzheimer's Disease Neuroimaging Initiative. (2020). A computational anatomy toolbox for the analysis of structural MRI data. *NeuroImage*, *2016*, 336–348.

Gaser, C., & Kurth, F. (2020). *Manual computational anatomy toolbox- cat12* (pp. 1–66). Structural Brain Mapping Group at the Departments of Psychiatry and Neurology, University of Jena.

Glasofer, D. R., Brown, A. J., & Riegel, M. (2015). Structured clinical interview for DSM-IV (SCID). In T. Wade (Ed.), *Encyclopedia of feeding and eating disorders* (pp. 1–4). Springer. https://doi.org/10.1007/978-981-287-087-2_80-1

Grahn, J. A., Parkinson, J. A., & Owen, A. M. (2008). The cognitive functions of the caudate nucleus. *Progress in Neurobiology*, *86*(3), 141–155. https://doi.org/10.1016/j.pneurobio.2008.09.004

Gupta, C. N., Calhoun, V. D., Rachakonda, S., Chen, J., Patel, V., Liu, J., Segall, J., Franke, B., Zwiers, M. P., Arias-Vasquez, A., Buitelaar, J., Fisher, S. E., Fernandez, G., van Erp, T. G., Potkin, S., Ford, J., Mathalon, D., McEwen, S., Lee, H. J., … Turner, J. A. (2015). Patterns of gray matter abnormalities in schizophrenia based on an international mega-analysis. *Schizophrenia Bulletin*, *41*(5), 1133–1142. https://doi.org/10.1093/schbul/sbu177

Haijma, S. V., Van Haren, N., Cahn, W., Koolschijn, P. C., Hulshoff Pol, H. E., & Kahn, R. S. (2013). Brain volumes in schizophrenia: A meta-analysis in over 18 000 subjects. *Schizophrenia Bulletin*, *39*(5), 1129–1138. https://doi.org/10.1093/schbul/sbs118

Hulshoff Pol, H. E., Schnack, H. G., Mandl, R. C., Cahn, W., Collins, D. L., Evans, A. C., & Kahn, R. S. (2004). Focal white matter density changes in schizophrenia: Reduced inter-hemispheric connectivity. *NeuroImage*, *21*(1), 27–35. https://doi.org/10.1016/j.neuroimage.2003.09.026

Jiang, J., Beck, J., Heller, K., & Egner, T. (2015). An insula-frontostriatal network mediates flexible cognitive control by adaptively predicting changing control demands. *Nature Communications*, *6*, 8165. https://doi.org/10.1038/ncomms9165

Jirsaraie, R. J., Sheffield, J. M., & Barch, D. M. (2018). Neural correlates of global and specific cognitive deficits in schizophrenia. *Schizophrenia Research*, *201*, 237–242. https://doi.org/10.1016/j.schres.2018.06.017

Kim, C., Johnson, N. F., Cilles, S. E., & Gold, B. T. (2011). Common and distinct mechanisms of cognitive flexibility in prefrontal cortex. *The Journal of Neuroscience*, *31*(13), 4771–4779. https://doi.org/10.1523/JNEUROSCI.5923-10.2011

Klune, C. B., Jin, B., & DeNardo, L. A. (2021). Linking mPFC circuit maturation to the developmental regulation of emotional memory and cognitive flexibility. *eLife*, *10*, e64567. https://doi.org/10.7554/eLife.64567

Koo, M. S., Levitt, J. J., McCarley, R. W., Seidman, L. J., Dickey, C. C., Niznikiewicz, M. A., Voglmaier, M. M., Zamani, P., Long, K. R., Kim, S. S., & Shenton, M. E. (2006). Reduction of caudate nucleus volumes in neuroleptic-naive female subjects with schizotypal personality disorder. *Biological Psychiatry*, *60*(1), 40–48. https://doi.org/10.1016/j.biopsych.2005.09.028

Kreczmanski, P., Heinsen, H., Mantua, V., Woltersdorf, F., Masson, T., Ulfig, N., Schmidt-Kastner, R., Korr, H., Steinbusch, H. W., Hof, P. R., & Schmitz, C. (2007). Volume, neuron density and total neuron number in five subcortical regions in schizophrenia. *Brain*, *130*(Pt 3), 678–692. https://doi.org/10.1093/brain/awl386

Kumari, S., Malik, M., Florival, C., Manalai, P., & Sonje, S. (2017). An assessment of five (PANSS, SAPS, SANS, NSA-16, CGI-SCH) commonly used symptoms rating scales in schizophrenia and comparison to newer scales (CAINS, BNSS). *Journal of Addiction Research & Therapy*, *8*(3). https://doi.org/10.4172/2155-6105.1000324

Lepage, M., Bodnar, M., & Bowie, C. R. (2014). Neurocognition: Clinical and functional outcomes in schizophrenia. *Canadian Journal of Psychiatry*, *59*(1), 5–12. https://doi.org/10.1177/070674371405900103

Lieberman, M. D., & Cunningham, W. A. (2009). Type I and type II error concerns in fMRI research: re-balancing the scale. *Social Cognitive and Affective Neuroscience*, *4*(4), 423–428. https://doi.org/10.1093/scan/nsp052

McCutcheon, R. A., Abi-Dargham, A., & Howes, O. D. (2019). Schizophrenia, dopamine and the striatum: From biology to symptoms. *Trends in Neurosciences*, *42*(3), 205–220. https://doi.org/10.1016/j.tins.2018.12.004

Meram, E. D., Baajour, S., Chowdury, A., Kopchick, J., Thomas, P., Rajan, U., Khatib, D., Zajac-Benitez, C., Haddad, L., Amirsadri, A., Stanley, J. A., & Diwadkar, V. A. (2023). The topology, stability, and instability of learning-induced brain network repertoires in schizophrenia. *Network Neuroscience*, *7*(1), 184–212. https://doi.org/10.1162/netn_a_00278

Oishi, K., Faria, A., Jiang, H., Li, X., Akhter, K., Zhang, J., Hsu, J. T., Miller, M. I., van Zijl, P. C., Albert, M., Lyketsos, C. G., Woods, R., Toga, A. W., Pike, G. B., Rosa-Neto, P., Evans, A., Mazziotta, J., & Mori, S. (2009). Atlas-based whole brain white matter analysis using large deformation diffeomorphic metric mapping: Application to normal elderly and Alzheimer's disease participants. *NeuroImage*, *46*(2), 486–499. https://doi.org/10.1016/j.neuroimage.2009.01.002

Oliver, L. D., Hawco, C., Homan, P., Lee, J., Green, M. F., Gold, J. M., DeRosse, P., Argyelan, M., Malhotra, A. K., Buchanan, R. W., Voineskos, A. N., & Group, S. (2021). Social cognitive networks and social cognitive performance across individuals with schizophrenia Spectrum disorders and healthy control participants. *Biological Psychiatry: Cognitive Neuroscience and Neuroimaging*, *6*(12), 1202–1214. https://doi.org/10.1016/j.bpsc.2020.11.014

O'Reilly, R. C. (2006). Biologically based computational models of high-level cognition. *Science*, *314*(5796), 91–94. https://doi.org/10.1126/science.1127242

Patton, J. H., Stanford, M. S., & Barratt, E. S. (1995). Factor structure of the Barratt impulsiveness scale. *Journal of Clinical Psychology*, *51*(6), 768–774. https://doi.org/10.1002/1097-4679(199511)51:6<768::aid-jclp2270510607>3.0.co;2-1

Perez-Costas, E., Melendez-Ferro, M., & Roberts, R. C. (2010). Basal ganglia pathology in schizophrenia: Dopamine connections and anomalies. *Journal of Neurochemistry*, *113*(2), 287–302. https://doi.org/10.1111/j.1471-4159.2010.06604.x

Pomarol-Clotet, E., Canales-Rodriguez, E. J., Salvador, R., Sarro, S., Gomar, J. J., Vila, F., Ortiz-Gil, J., Iturria-Medina, Y., Capdevila, A., & McKenna, P. J. (2010). Medial prefrontal cortex pathology in schizophrenia as revealed by convergent findings from multimodal imaging. *Molecular Psychiatry*, *15*(8), 823–830. https://doi.org/10.1038/mp.2009.146

Schaum, M., Pinzuti, E., Sebastian, A., Lieb, K., Fries, P., Mobascher, A., Jung, P., Wibral, M., & Tuscher, O. (2021). Right inferior frontal gyrus implements motor inhibitory control via beta-band oscillations in humans. *eLife*, *10*, e61679. https://doi.org/10.7554/eLife.61679

Schiffer, A. M., & Schubotz, R. I. (2011). Caudate nucleus signals for breaches of expectation in a movement observation paradigm. *Frontiers in Human Neuroscience*, *5*, 38. https://doi.org/10.3389/fnhum.2011.00038

Schroder, J., Niethammer, R., Geider, F. J., Reitz, C., Binkert, M., Jauss, M., & Sauer, H. (1991). Neurological soft signs in schizophrenia. *Schizophrenia Research*, *6*(1), 25–30. https://doi.org/10.1016/0920-9964(91)90017-l

Scott, J. G., & Berger, J. O. (2006). An exploration of aspects of Bayesian multiple testing. *Journal of Statistical Planning and Inference*, *136*(7), 2144–2162. https://doi.org/10.1016/j.jspi.2005.08.031

Sharp, D. J., Bonnelle, V., De Boissezon, X., Beckmann, C. F., James, S. G., Patel, M. C., & Mehta, M. A. (2010). Distinct frontal systems for response inhibition, attentional capture, and error processing. *Proceedings of the National Academy of Sciences of the United States of America*, *107*(13), 6106–6111. https://doi.org/10.1073/pnas.1000175107

Sheffield, J. M., Repovs, G., Harms, M. P., Carter, C. S., Gold, J. M., MacDonald, A. W., 3rd, Daniel Ragland, J., Silverstein, S. M., Godwin, D., & Barch, D. M. (2015). Fronto-parietal and cingulo-opercular network integrity and cognition in health and schizophrenia. *Neuropsychologia*, *73*, 82–93. https://doi.org/10.1016/j.neuropsychologia.2015.05.006

Shepherd, A. M., Laurens, K. R., Matheson, S. L., Carr, V. J., & Green, M. J. (2012). Systematic meta-review and quality assessment of the structural brain alterations in schizophrenia. *Neuroscience and Biobehavioral Reviews*, *36*(4), 1342–1356. https://doi.org/10.1016/j.neubiorev.2011.12.015

Sigmundsson, T., Suckling, J., Maier, M., Williams, S., Bullmore, E., Greenwood, K., Fukuda, R., Ron, M., & Toone, B. (2001). Structural abnormalities in frontal, temporal, and limbic regions and interconnecting white matter tracts in schizophrenic patients with prominent negative symptoms. *The American*

Journal of Psychiatry, *158*(2), 234–243. https://doi.org/10.1176/appi.ajp.158.2.234

Simpson, E. H., Kellendonk, C., & Kandel, E. (2010). A possible role for the striatum in the pathogenesis of the cognitive symptoms of schizophrenia. *Neuron*, *65*(5), 585–596. https://doi.org/10.1016/j.neuron.2010.02.014

Snodgrass, J. G., & Corwin, J. (1988). Pragmatics of measuring recognition memory: Applications to dementia and amnesia. *Journal of Experimental Psychology. General*, *117*(1), 34–50. https://doi.org/10.1037//0096-3445.117.1.34

Standke, I., Trempler, I., Dannlowski, U., Schubotz, R. I., & Lencer, R. (2021). Cerebral and behavioral signs of impaired cognitive flexibility and stability in schizophrenia spectrum disorders. *NeuroImage: Clinical*, *32*, 102855. https://doi.org/10.1016/j.nicl.2021.102855

Trempler, I., Binder, E., El-Sourani, N., Schiffler, P., Tenberge, J. G., Schiffer, A. M., Fink, G. R., & Schubotz, R. I. (2018). Association of grey matter changes with stability and flexibility of prediction in akinetic-rigid Parkinson's disease. *Brain Structure & Function*, *223*(5), 2097–2111. https://doi.org/10.1007/s00429-018-1616-2

Trempler, I., Burkner, P. C., El-Sourani, N., Binder, E., Reker, P., Fink, G. R., & Schubotz, R. I. (2020). Impaired context-sensitive adjustment of behaviour in Parkinson's disease patients tested on and off medication: An fMRI study. *NeuroImage*, *212*, 116674. https://doi.org/10.1016/j.neuroimage.2020.116674

Trempler, I., Schiffer, A. M., El-Sourani, N., Ahlheim, C., Fink, G. R., & Schubotz, R. I. (2017). Frontostriatal contribution to the interplay of flexibility and stability in serial prediction. *Journal of Cognitive Neuroscience*, *29*(2), 298–309. https://doi.org/10.1162/jocn_a_01040

van Doorn, J., van den Bergh, D., Bohm, U., Dablander, F., Derks, K., Draws, T., Etz, A., Evans, N. J., Gronau, Q. F., Haaf, J. M., Hinne, M., Kucharsky, S., Ly, A., Marsman, M., Matzke, D., Gupta, A., Sarafoglou, A., Stefan, A., Voelkel, J. G., & Wagenmakers, E. J. (2021). The JASP guidelines for conducting and reporting a Bayesian analysis. *Psychonomic Bulletin & Review*, *28*(3), 813–826. https://doi.org/10.3758/s13423-020-01798-5

van Haren, N. E., Hulshoff Pol, H. E., Schnack, H. G., Cahn, W., Mandl, R. C., Collins, D. L., Evans, A. C., & Kahn, R. S. (2007). Focal gray matter changes in schizophrenia across the course of the illness: A 5-year follow-up study. *Neuropsychopharmacology*, *32*(10), 2057–2066. https://doi.org/10.1038/sj.npp.1301347

Veijola, J., Guo, J. Y., Moilanen, J. S., Jaaskelainen, E., Miettunen, J., Kyllonen, M., Haapea, M., Huhtaniska, S., Alaraisanen, A., Maki, P., Kiviniemi, V., Nikkinen, J., Starck, T., Remes, J. J., Tanskanen, P., Tervonen, O., Wink, A. M., Kehagia, A., Suckling, J., … Murray, G. K. (2014). Longitudinal changes in total brain volume in schizophrenia: Relation to symptom severity, cognition and antipsychotic medication. *PLoS One*, *9*(7), e101689. https://doi.org/10.1371/journal.pone.0101689

Wager, T. D., Spicer, J., Insler, R., & Smith, E. E. (2014). The neural bases of distracter-resistant working memory. *Cognitive, Affective, & Behavioral Neuroscience*, *14*(1), 90–105. https://doi.org/10.3758/s13415-013-0226-y

Walterfang, M., Wood, S. J., Velakoulis, D., & Pantelis, C. (2006). Neuropathological, neurogenetic and neuroimaging evidence for white matter pathology in schizophrenia. *Neuroscience and Biobehavioral Reviews*, *30*(7), 918–948. https://doi.org/10.1016/j.neubiorev.2006.02.001

Wang, Y., Ma, N., He, X., Li, N., Wei, Z., Yang, L., Zha, R., Han, L., Li, X., Zhang, D., Liu, Y., & Zhang, X. (2017). Neural substrates of updating the prediction through prediction error during decision making. *NeuroImage*, *157*, 1–12. https://doi.org/10.1016/j.neuroimage.2017.05.041

Williams, L. M. (2008). Voxel-based morphometry in schizophrenia: Implications for neurodevelopmental connectivity models, cognition and affect. *Expert Review of Neurotherapeutics*, *8*(7), 1049–1065. https://doi.org/10.1586/14737175.8.7.1049

Wilmsmeier, A., Ohrmann, P., Suslow, T., Siegmund, A., Koelkebeck, K., Rothermundt, M., Kugel, H., Arolt, V., Bauer, J., & Pedersen, A. (2010). Neural correlates of set-shifting: Decomposing executive functions in schizophrenia. *Journal of Psychiatry & Neuroscience*, *35*(5), 321–329. https://doi.org/10.1503/jpn.090181

Woo, C. W., Krishnan, A., & Wager, T. D. (2014). Cluster-extent based thresholding in fMRI analyses: Pitfalls and recommendations. *NeuroImage*, *91*, 412–419. https://doi.org/10.1016/j.neuroimage.2013.12.058

Zhang, X., Zhang, Y., Liao, J., Jiang, S., Yan, J., Yue, W., Zhang, D., & Yan, H. (2018). Progressive Grey matter volume changes in patients with schizophrenia over 6 weeks of antipsychotic treatment and their relationship to clinical improvement. *Neuroscience Bulletin*, *34*(5), 816–826. https://doi.org/10.1007/s12264-018-0234-6

How to cite this article: Herkströter, F., Zahedi, A., Standke, I., Dannlowski, U., Lencer, R., Schubotz, R. I., & Trempler, I. (2024). Gray matter matters: Cognitive stability and flexibility in schizophrenia spectrum disorder. *Psychophysiology*, *00*, e14596. https://doi.org/10.1111/psyp.14596

APPENDIX A

TABLE A1 Brain areas that showed significant atrophy in SZ patients compared to healthy controls.

Test statistic	*X* (mm)	*Y* (mm)	*Z* (mm)	p^{a}-value $\times 10^{-5}$	*t*-values[a]	Cluster size (*K*)
Lingual gyrus	−6	−76.5	−3	0.177	5.39	2828
Inferior occipital gyrus	−40.5	−91.5	−7.5	3.71	4.42	648
Posterior middle frontal gyrus	33	18	33	6.68	4.23	462
Inferior temporal gyrus	46.5	−54	−1.5	17	3.92	215
Middle occipital gyrus	37.5	−78	19.5	17.5	3.91	264
Middle occipital gyrus	−36	−73.5	24	22.3	3.83	340
Amygdala extending into hippocampus proper	−30	−4.5	−22.5	23	3.82	958
Inferior temporal sulcus	−52.5	−45	−15	28.3	3.75	267
Parietal operculum/insula	49.5	−1.5	4.5	40.8	3.62	425
Thalamus (WM)	13.5	−9	18	43.2	3.60	154
Posterior hippocampus	21	−37.5	−4.5	62	3.48	365
Middle frontal gyrus	36	39	21	64.3	3.46	110
Parietal operculum	−46.5	−36	31.5	91.3	3.34	231
Inferior temporal gyrus	51	−55.5	−15	169	3.12	82
Ventromedial-orbitofrontal cortex	0	45	−25.5	183.4	3.09	80

Note: The whole brain analysis threshold was $p < .005$, *contigueous voxels* > 80, which is chosen based on the suggestions of Woo et al. (2014), to enhance spatial localization and interpretability.

Abbreviations: mm, millimeter; SZ, schizophrenia spectrum disorders.

[a]Presented *p* and *t*-values are related to the peak of the cluster. For readability, *p*-values are transformed (p-value $\times 10^{-5}$).

APPENDIX B

TABLE A2 Voxel-based morphometry results of a-priori-defined anatomical ROIs for patients only.

Response	Coefficient	Estimate [95% C.I.]	*E.E.*	Hypothesis	*p.p.*	*B.F.*
mPFC	CPZ	−0.0008 [−0.001, 0.002]	0.0007	CPZ = 0	**>.999**	**6890**
	TIV	0.01 [0.009, 0.017]	0.002	TIV > 0	**>.999**	**>9999**
	Age	−0.13 [−0.19, −0.08]	0.04	Age < 0	**>.999**	**1499**
	Gender	−0.68 [−2.37, 0.97]	0.84	Gender = 0	.89	**8.24**
IFG	CPZ	−0.0003 [−0.001, 0.001]	0.0005	CPZ = 0	**>.999**	**>9999**
	TIV	0.004 [0.002, 0.007]	0.001	TIV > 0	**.998**	**520.7**
	Age	−0.09 [−0.13, −0.05]	0.02	Age < 0	**>.999**	**1499**
	Gender	−0.05 [−1.14, 1.04]	0.55	Gender = 0	**.95**	**18.75**
CN	CPZ	−0.0001 [−0.001, 0.001]	0.0001	CPZ = 0	**>.999**	**>9999**
	TIV	0.001 [0.0004, 0.002]	0.0004	TIV > 0	**.994**	**168.01**
	Age	−0.01 [−0.02, −0.01]	0.01	Age < 0	**.95**	**17.21**
	Gender	0.01 [−0.23, 0.42]	0.16	Gender = 0	**.98**	**52.05**
Putamen	CPZ	−0.0001 [−0.001, 0.001]	0.0002	CPZ = 0	**>.999**	**>9999**
	TIV	0.001 [0.00, 0.002]	0.0007	TIV > 0	.94	**15.99**
	Age	−0.01 [−0.03, 0.00]	0.01	Age < 0	.92	**10.92**
	Gender	0.18 [−0.31, 0.68]	0.25	Gender = 0	**.97**	**31.88**

Note: Highlighted Bayes factor and posterior probabilities show at least substantial evidence supporting the tested hypothesis (van Doorn et al., 2021).

Abbreviations: B.F., Bayes Factor; C.I., credential interval; CN, caudate nucleus; E.E., estimation error; IFG, inferior frontal gyrus; mPFC, medial prefrontal cortex; p.p., posterior probability; SZ, schizophrenia spectrum disorder.

APPENDIX C

TABLE A3 Voxel-based morphometry results of left and right IFG ROIs.

Response	Coefficient	Estimate [95% C.I.]	*E.E.*	Hypothesis	*p.p.*	*B.F.*
Right IFG	Hits	3.9 [1.69, 6.13]	1.13	Hits = 0	**.02**	**0.02**
	CRs	1.37 [−2.57, 5.89]	2.13	CRs = 0	.77	**3.27**
	Group	0.99 [0, 2.02]	0.04	Group = 0	**.97**	**32.58**
Left IFG	Hits	3.2 [0.96, 5.11]	1.05	Hits = 0	.16	**0.14**
	CRs	0.97 [−3.04, 4.89]	2.02	CRs = 0	.82	**4.58**
	Group	0.36 [−0.59, 1.32]	0.49	Group = 0	**.99**	**157.63**

Note: Highlighted Bayes factor and posterior probabilities show at least substantial evidence supporting the tested hypothesis (van Doorn et al., 2021). The model used was: $(GMV_{mPFC}, GMV_{right\_IFG}, GMV_{left\_IFG}, GMV_{CN}, GMV_{putamen}) \sim CRs + Hits + Group$.

Abbreviations: B.F., Bayes Factor; C.I., credential interval; E.E., estimation error; IFG, inferior frontal gyrus; p.p., posterior probability; SZ, schizophrenia spectrum disorder.